

UC Berkeley

Working Papers

Title

Dynamic Modeling Of Tractor-semitrailer Vehicles In Automated Highway Systems

Permalink

<https://escholarship.org/uc/item/4cd4x08c>

Authors

Chen, Chieh
Tomizuka, Masayoshi

Publication Date

1995

CALIFORNIA PATH PROGRAM
INSTITUTE OF TRANSPORTATION STUDIES
UNIVERSITY OF CALIFORNIA, BERKELEY

Dynamic Modeling of Tractor-Semitrailer Vehicles in Automated Highway Systems

Chieh Chen

Masayoshi Tomizuka

Department of Mechanical Engineering
University of California, Berkeley

California PATH Working Paper

UCB-ITS-PWP-95-8

This work was performed as part of the California PATH Program of the University of California, in cooperation with the State of California Business, Transportation, and Housing Agency, Department of Transportation; and the United States Department Transportation, Federal Highway Administration.

The contents of this report reflect the views of the authors who are responsible for the facts and the accuracy of the data presented herein. The contents do not necessarily reflect the official views or policies of the State of California. This report does not constitute a standard, specification, or regulation.

July 1995

ISSN 1055-1417

Dynamic Modeling of Tractor-Semitrailer Vehicles for Automated Highway Systems

Chieh Chen and Masayoshi Tomizuka

Department of Mechanical Engineering
University of California at Berkeley
Berkeley, California 94720

Abstract

This report is concerned with dynamic modeling of the tractor-semitrailer vehicles in Automated Highway Systems (AHS). A modeling approach for roll, pitch and yaw motions of tractor-semitrailer vehicles is proposed. A coordinate system is defined to precisely describe the translational and rotational motions of the vehicle. A nonlinear complex model and simplified models for designing controller will be proposed.

A simplified linear model, which includes lateral and yaw motions, is derived based on the assumptions that the longitudinal velocity is constant and that the vehicle lateral and yaw motions are small. It is shown that the vehicle damping is inversely proportional to the longitudinal speed, and the gyroscopic forces are proportional to the product of trailer mass and the longitudinal speed.

Keywords

Vehicle dynamics, Lateral Control, Automated Highway Systems

Executive Summary

This report summarizes the first year research results of the PATH project (MOU 129) : Steering and Braking Control of Heavy Duty Vehicles. This project is concerned with the dynamic modeling and lateral motion control of heavy-duty vehicles in automated highway systems. The objectives of this research are to characterize the dynamic response of articulated heavy-duty vehicles, identify the key system parameters, develop control algorithms to achieve automatic guidance, and conduct experiments on lateral guidance control of articulated heavy-duty vehicles.

A modeling approach for roll, pitch and yaw motions of articulated heavy-duty vehicles is described in this report. A coordinate system is defined to precisely describe the translational and rotational motions of the vehicle. A nonlinear complex model is proposed to simulate the dynamic responses of articulated vehicles and will be exploited to evaluate the effectiveness of lateral control algorithms in the second and third years. This simulation model is derived by applying Lagrangian mechanics and has an advantage over a Newtonian mechanics formulation in that our models eliminate the holonomic constraints at the fifth wheel by carefully choosing the generalized coordinates. Since there is no constraint involved in the equations of motion, it is easier to design control algorithms and to solve the differential equations numerically. Other configurations of articulated vehicles, for example tractor/three trailer combination, can also be modeled with the same approach. A linear control model is simplified from the complex nonlinear model. The directional response of the complex model and that of the simplified model are compared. Linear quadratic optimal controller as well as optimal preview controller will be designed based on this linear model in the near future.

1 Introduction

In the past few years, there has been an increasing amount of research on Advanced Vehicle Control Systems (AVCS) for Automated Highway Systems (AHS). In the area of automated vehicle lateral control, Zhang (1991) has proposed a magnetic marker referencing/sensing system which accurately measures vehicle lateral displacement from the road centerline. Peng and Tomizuka (1991) synthesized a preview optimal control algorithm for light passenger vehicles based on a fourth order linear model. This algorithm has been validated by an experimental study (Peng et al. 1992). A fuzzy rule-based controller for vehicle lateral guidance has been designed (Hessburg and Tomizuka 1993). Lane change maneuvers (Chee and Tomizuka 1994) in automated highway systems are also currently being studied. However, these researches are all concerned with the control of passenger vehicles. On the other hand, heavy duty vehicles play an important role in transportation. The roadway transportation system of the United States includes 190 million motor vehicles, more than 45 million of which are trucks and buses (MVMA 1992). In 1987, buses, single-unit and articulated trucks were responsible for 28.5% of the total motor vehicle travel miles (MVMA 1987), which is significantly higher than the 22.8% of 1979. Nevertheless, only a very small fraction of past AVCS research was devoted to the control of heavy vehicles for automated highway systems.

The directional response of articulated heavy duty vehicles is quite different from that of passenger vehicles in several ways. First, articulated heavy duty vehicles are usually heavier, more likely to bear nonlinear dynamics due to tires, articulation joints and suspension systems, and respond slower to steering inputs than passenger vehicles. Secondly, variations of parameters, such as mass, moment of inertia and location of mass center due to trailer load condition, are much larger than those in passenger vehicles. Thirdly, articulated heavy duty vehicles exhibit a roll instability mode due to high location of the mass center. In a recent study (Huang et al. 1993), it was found that roll motion has to be included for accurate modeling even for minivan types of vehicles. Fourthly, articulated vehicles are prone to unstable yaw modes. There are two yaw instability modes studied in the past: divergent yaw response (jackknifing and trailer swing) and (lightly damped) nondivergent rearward amplification (fishtailing). Jackknifing is one of the most common causes of serious traffic accidents of articulated vehicles. The principal mechanism causing divergent yaw instability was found to be tire force saturation, which may be caused directly by braking or indirectly by steering inputs. Excessive steering inputs may cause roll motions that reduce the tire force capacity on one side of the vehicle and result in tire force saturation. Fifthly, the off-tracking phenomenon in articulated vehicles is more significant than in passenger vehicles. Off-tracking is defined as the radial difference between the path of the front-most wheel and that of the rear-most wheel. A significant amount of knowledge has been accumulated on the dynamics of articulated vehicles (Dugoff and Murphy 1971; Vlk 1982; Vlk 1985). However, little effort has been applied toward their control, especially for automatic guidance purposes. Utilizing modern control technologies, the automatically guided heavy duty vehicles can avoid these unstable modes, which may occur in improper human maneuvers.

This report is concerned with dynamic modeling of articulated tractor-semitrailer vehicles in Automated Highway Systems (AHS). Firstly, a complex nonlinear simulation model for the tractor semitrailer vehicle is proposed. This model includes the roll, pitch and yaw motions of tractor and semitrailer. This model will be used to validate the effectiveness of lane following control algorithms designed based on simplified models. The uniqueness of this model is that we derive the equations of motion by applying Lagrangian mechanics. Lagrangian mechanics formulation has the advantage over Newtonian mechanics in that it can eliminate the holonomic constraints at the linking joint between tractor and semitrailer by carefully choosing the generalized coordinates. The Lagrangian mechanics formulation is particularly suitable for control algorithm synthesis. Secondly, a 3 degree of freedom (6 states) linear control model including the vehicle lateral motion as well as tractor's and semitrailer's yaw motions is obtained by simplifying the nonlinear complex model. Some linear analysis shows that the system damping is inversely proportional to the vehicle longitudinal speed. This result generalizes Bundorf's analysis (1967) which showed that the damping of the motion of the articulation angle is inversely proportional to the vehicle speed by neglecting the interaction of tractor and trailer. Strong gyroscopic effect can also be seen in this linear model. The gyroscopic terms are proportional to trailer's mass times vehicle speed.

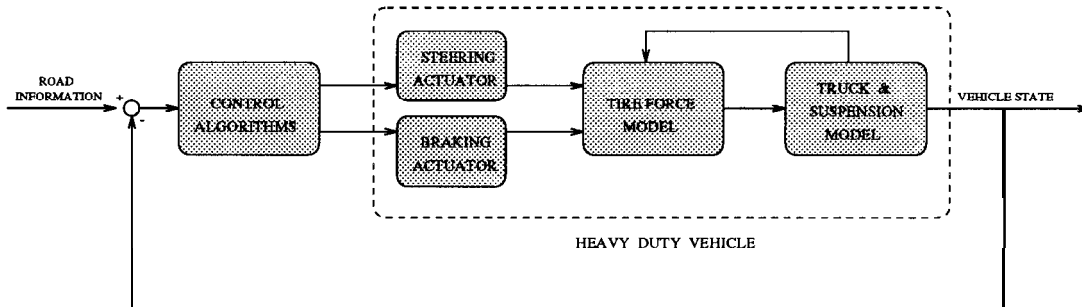


Figure 1: Automated Vehicle System

2 Dynamic Modeling of Articulated Vehicles

2.1 Definition of Coordinate Systems and Equations of Motion

A coordinate system (figure 2) is defined to precisely describe the translational and rotational motion of the vehicle. $X_n Y_n Z_n$ is the inertial reference coordinate. We will obtain the expressions of vehicle's kinetic and potential energies relative to this reference coordinate. $X_u Y_u Z_u$ is the tractor's unsprung mass coordinate.

a There is relative translational motion in the $X - Y$ plane and relative rotational yaw motion in the direction of Z axis between $X_n Y_n Z_n$ and $X_u Y_u Z_u$. $X_s Y_s Z_s$ is the tractor's sprung mass coordinate, which is body-fixed at the tractor's center of mass. Coordinate $X_s Y_s Z_s$ has roll and pitch motions relative to

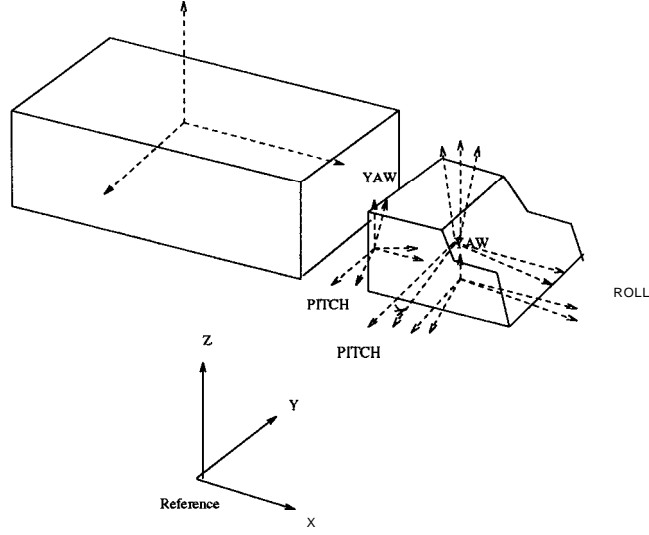


Figure 2: Coordinate System to Describe the Vehicle Motion

coordinate $X_u Y_u Z_u$. Since roll and pitch motions are small in normal highway maneuvers, we will not define Euler angles to describe them. These two coordinates, $X_u Y_u Z_u$ and $X_s Y_s Z_s$, can be used to completely describe the tractor's translational and rotational motions relative to the inertial coordinate $X_n Y_n Z_n$. To describe the semitrailer's motion, we need to study the linking mechanism between tractor and semitrailer first. The most common joint of tractor semitrailer vehicle is called the "fifth wheel" (figure 3) (Ellis 1989). The kinematic design of the fifth wheel provides for free articulation in yaw mode while connecting tractor and semitrailer in translational motion. The pitch and roll connections between tractor and semitrailer are more complicated. We examine two extreme cases: 1. When the articulation angle is 0 degrees, the fifth wheel provides free pitch between tractor and semitrailer, while the roll motion is rigidly connected. 2. When the articulation angle is 90 degrees, the tractor's pitch and trailer's roll motions are free, while the tractor's roll and trailer's pitch motions are rigidly connected. From this, we see that the fifth wheel imposes three translational motion constraints and one combined roll and pitch rotational motion constraint. Since the trailer has six degree of freedom and the fifth wheel provides 4 degree of freedom constraints, we only need to choose another two generalized coordinates to describe the trailer's motion. The most natural way is to attach two coordinates $X_{yf} Y_{yf} Z_{yf}$, $X_{pf} Y_{pf} Z_{pf}$ satisfying the kinematic constraints at the fifth wheel. $X_{pf} Y_{pf} Z_{pf}$ has the relative pitch motion to $X_s Y_s Z_s$, while $X_{yf} Y_{yf} Z_{yf}$ has relative yaw motion to $X_{pf} Y_{pf} Z_{pf}$. Having completely defined the coordinate system, we can calculate the kinetic energy, T , and potential energy, V , of the vehicle. The equations of motion can then be derived by applying Lagrange's equations, $\frac{d}{dt} \frac{\partial L}{\partial \dot{q}} - \frac{\partial L}{\partial q} = F_g$, where $L = T - V$ is the Lagrangian and F_g is the generalized force. The transformation matrices between each coordinate and kinetic and potential energies are listed in Appendix

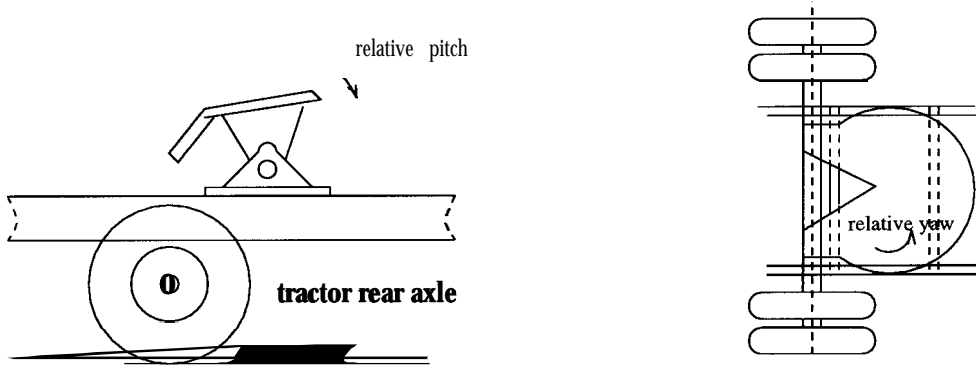


Figure 3: The mechanism of 'fifth wheel'

Here we assume that vehicle body is rigid, i.e., we neglect the compliant effect of the vehicle body. This assumption can be relaxed by introducing another two coordinates for the tractor-semitrailer vehicle: one, say X_s, Y_s, Z_s , is body-fixed at the tractor's fifth wheel, and the other, say X_{s2}, Y_{s2}, Z_{s2} , is body fixed at trailer's center of mass. Coordinate X_s, Y_s, Z_s has relative roll motion to coordinate X_s, Y_s, Z_s ; similarly, coordinate X_{s2}, Y_{s2}, Z_{s2} has relative roll motion to coordinate X_{yf}, Y_{yf}, Z_{yf} . The vehicle body can be modeled as a combination of a spring and a damper. Knowing the spring stiffness and damping coefficient, we can calculate the Lagrangian again as well as the equations governing the tractor's and semitrailer's body vibrational modes.

2.2 Generalized Forces

The external forces acting on the vehicle body are from the tire/road interface and suspensions. In applying Lagrange's equations, we need to calculate each generalized force corresponding to each generalized coordinate explicitly, i.e., we want to transform the external forces in the Cartesian coordinate to the generalized force corresponding to each generalized coordinate. Figure 4 shows the definition of the number of the vehicle wheel and the external forces at wheel i in the Cartesian coordinate, where the longitudinal force, F_{Ai} , is in the direction of X_u axis, the lateral force, F_{Bi} , is in the direction of Y_u axis and the normal force, F_{Pi} , is in the direction of Z_u axis, $i = 1$ to 6.

Deriving the position vector in Cartesian coordinates of each wheel in terms of the generalized coordinates,

$$\vec{P}_{wi} = \begin{pmatrix} f_{wix}(x, y, z, \theta, \phi, \epsilon, \theta_f, \epsilon_f) \\ f_{wiy}(x, y, z, \theta, \phi, \epsilon, \theta_f, \epsilon_f) \\ f_{wiz}(x, y, z, \theta, \phi, \epsilon, \theta_f, \epsilon_f) \end{pmatrix} \quad (1)$$

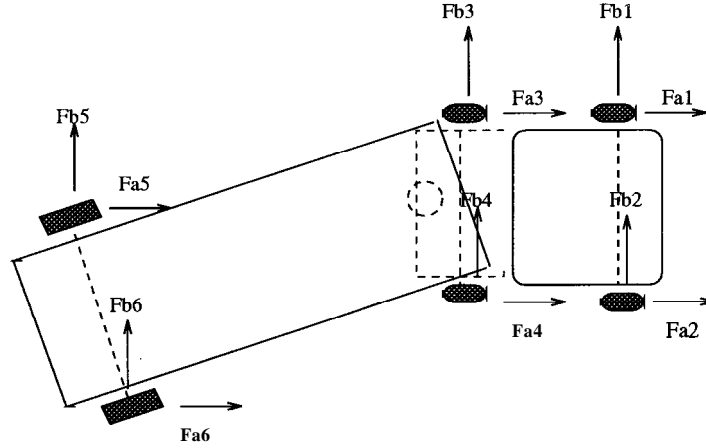


Figure 4: Definition of Tire Force in the Cartesian Coordinate

we can calculate the generalized forces as

$$Q_j = \sum_{i=1}^n F_i \frac{\partial x_i}{\partial q_j} \quad (2)$$

The expressions of the generalized forces are listed in appendix 3.

3 Subsystems : Tire Force Model and Suspension Model

3.1 Tire Force Model

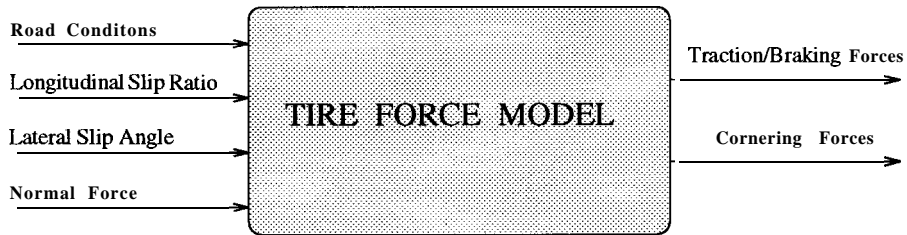


Figure 5: Tire Force Model

Since all forces acting on the vehicle body are from tire/road interfaces and through the vehicle's suspension system, an accurate tire force model to predict tire traction/baking force and cornering force is crucial for the dynamic modeling and response of the vehicle.

There are two common approaches to the tire force modeling. 1. Curve-fitting of the experimental data. This approach can predict a more accurate force traction field; however, the data depends on tire types;

thus it is less portable. 2. Analytical tire model. One way to analyze the traction field is to divide the tire contact patch into two zones: the sliding zone and the adhesion zone. Shear stresses in the sliding zone of the contact patch are determined by the frictional properties of the tire/road interface. Shear stresses in the adhesion zone are determined by the elastic properties of the tire; for example, the cornering stiffness C_α and longitudinal stiffness C_s represent the first order approximation of tire force elastic properties. We adopt the second approach at this stage of research and use the tire model by Baraket and Fancher (1989) in the simulation model. The structure of this tire model is summarized in figure 6.

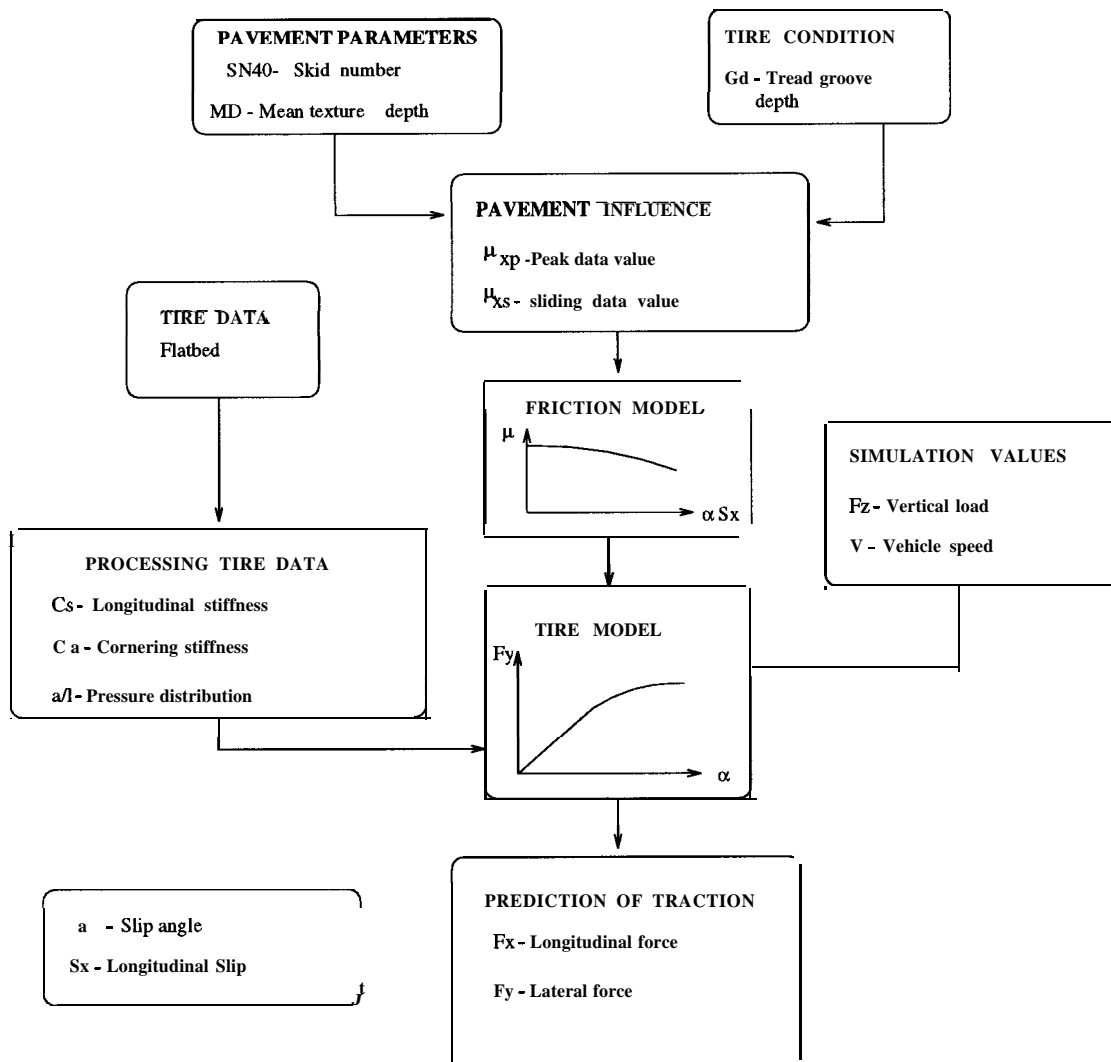


Figure 6: Comprehensive Tire Model (Baraket and Fancher)

To use this tire force model, tire longitudinal slip ratios and lateral slip angles in terms of vehicle states are calculated for 6-wheel tractor-semitrailer vehicles, which are listed in appendix 4.

For the steering controller design purpose, we can simplify the tire model (see figure 7) as

$$F_{xi} = C_{Si} \lambda_i \quad (3)$$

$$F_{yi} = C_{\alpha i} (\delta_i - \zeta_i) \quad (4)$$

where

F_{xi} is the longitudinal traction force;

F_{yi} is the cornering force;

C_{Si} is the longitudinal stiffness;

λ_i is the longitudinal slip at i -th wheel;

$C_{\alpha i}$ is the cornering stiffness at i -th wheel;

δ_i is the front wheel steering angle and

ζ_i is the vehicle slip angle at i -th wheel.

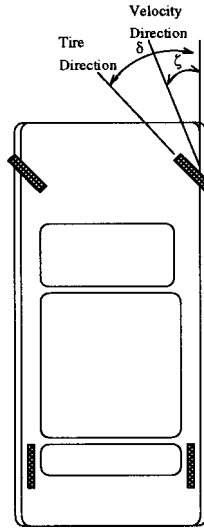


Figure 7: Simplified Tire Model

3.2 Suspension Model

By far the majority of commercial vehicle suspensions employ the leaf spring (SAE 1982) as the vertically compliant element. Instead of using experimental suspension data, we will adopt an analytical approach to model the suspension as the combination of spring element, damper element and Coulomb friction element. As shown in figure 8, the vertical force acting on the vehicle sprung mass through the suspension system is equal to the static equilibrium force plus the perturbation force, F_s , from the spring equilibrium point. The perturbation force can be calculated as

$$F_{si} = F_c \text{sgn}(\dot{e}_i) + K e_i + D \dot{e}_i, \quad (5)$$

where

e_i is the deflection of the i -th spring from its equilibrium position;

F_c is the coulumb friction;

K is the spring stiffness and

D is the damping ratio.

The expression of each e_i is listed in appendix 5.

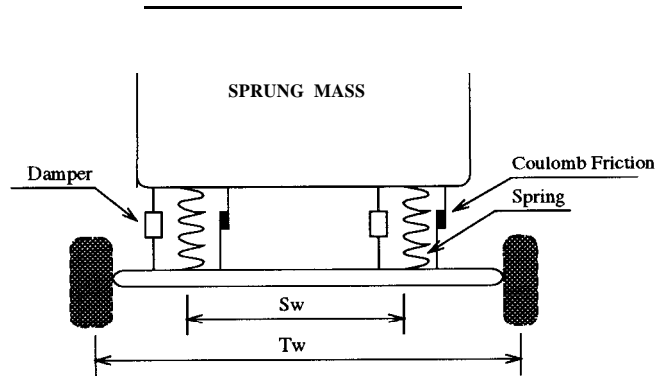


Figure 8: Suspension Model

4 Linear Analysis

4.1 Linearization of the Equations of Motion

Since the dynamic model developed in section 2 and section 3 is too complicated for analysis of the system characteristics and design of a path tracking controller, we will ignore some high frequency dynamics and linearize the equations of motion. Linearization of the equations of motion is reasonable because the vehicle lateral and yaw motions are small in normal highway maneuvers. We assume that

- The pitch and roll motions are small and therefore negligible
- The lateral and yaw motions, $y, \dot{y}, \epsilon, \dot{\epsilon}, \epsilon_f, \dot{\epsilon}_f$, are small.
- Second and higher order terms involving small quantities can be ignored.
- Forward velocity of the tractor (\dot{x}) remains constant.
- Tire cornering force is propotional to the lateral slip angle. (The propotional constant is the tire cornering stiffness, C_α .)

Then, we get a 3 degree of freedom (6 states) control model:

$$M\ddot{q} + C\dot{q} + G\dot{q} + Kq = D\delta \quad (6)$$

where

$$q = \begin{pmatrix} y \\ \epsilon \\ \epsilon_f \end{pmatrix} \quad (7)$$

$$M = \begin{pmatrix} m_1 + m_2 & -m_2(d_1 + d_3) & -m_2d_3 \\ -m_2(d_1 + d_3) & I_{z1} + I_{z2} + m_2(d_1 + d_3)^2 & I_{z2} + m_2d_3^2 + m_2d_1d_3 \\ -m_2d_3 & I_{z2} + m_2d_3^2 + m_2d_1d_3 & I_{z2} + m_2d_3^2 \end{pmatrix} \quad (8)$$

$$C = \frac{2}{\dot{x}} \begin{pmatrix} C_{\alpha f} + C_{\alpha r} + C_{\alpha t} & l_1C_{\alpha f} - l_2C_{\alpha r} - (l_3 + d_1)C_{\alpha t} & -l_3C_{\alpha t} \\ l_1C_{\alpha f} - l_2C_{\alpha r} - (l_3 + d_1)C_{\alpha t} & l_1^2C_{\alpha f} + l_2^2C_{\alpha r} + (2l_3 + d_1)^2C_{\alpha t} & l_3(l_3 + d_1)C_{\alpha t} \\ -l_3C_{\alpha t} & l_3(l_3 + d_1)C_{\alpha t} & l_3^2C_{\alpha t} \end{pmatrix} \quad (9)$$

$$G = \begin{pmatrix} 0 & 0 & 0 \\ 0 & 0 & m_2d_3\dot{x} \\ 0 & -m_2d_3\dot{x} & 0 \end{pmatrix} \quad (10)$$

$$K = \begin{pmatrix} 0 & 0 & -2C_{\alpha t} \\ 0 & 0 & 2(l_3 + d_1)C_{\alpha t} \\ 0 & 0 & 2l_3C_{\alpha t} \end{pmatrix} \quad (11)$$

and

$$D = \begin{pmatrix} 2C_{\alpha f} \\ 2l_1C_{\alpha f} \\ 0 \end{pmatrix} \quad (12)$$

Please refer to appendix 1 for the nomenclature.

We see from this simplified model that M is a symmetric positive definite matrix which contains all of the inertial information of the vehicle system. This property can be utilized in controller design. Also, the C matrix can be interpreted as a damping matrix. Each element of the C matrix contains the tire cornering stiffness. If the cornering stiffness is small, the vehicle system will become less damped and more oscillatory; for example, if the vehicle is operated on an icy road, the vehicle stability will decrease. We also see that the vehicle's longitudinal velocity \dot{x} appears in the denominator of the damping matrix; therefore the system damping is inversely proportional to the vehicle longitudinal velocity, which also agrees with our physical experience. Another interesting observation is that this system contains a skew-symmetric matrix G ; thus this system can be classified as a gyroscopic system. We see that the gyroscopic effect is proportional to the product of the longitudinal velocity and the mass of the semitrailer.

4.2 Change of Local Reference Coordinate

The above linearized model is referenced by the tractor's local unsprung mass coordinate. To design a lane following controller, we need to change the local reference coordinate from the tractor's unsprung mass coordinate to the coordinate sitting on the road center line. Thus the lateral displacement and relative yaw angle with respect to road center can be explicitly expressed. The road center coordinate $X_r Y_r Z_r$ is defined uniquely such that the X_r axis is tangent to the road center line and the Y_r axis passes through the tractor's center of mass as in figure 9, where y_r is the relative lateral displacement from the tractor's center of mass to the road center line and ϵ_r is the relative yaw angle of the tractor to the road center.

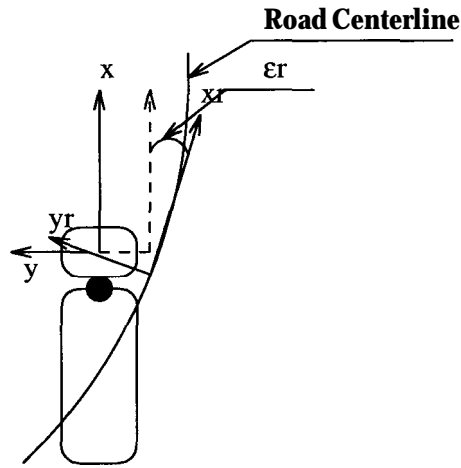


Figure 9: Local Reference Coordinate Transformation

Assume again that $y_r, \dot{y}_r, \epsilon_r$ and $\dot{\epsilon}_r$ are small. Some coordinate transformation analysis shows that

$$\dot{y} = \dot{y}_r - \dot{x}\epsilon_r \quad (13)$$

$$\ddot{y} = \ddot{y}_r - \dot{x}\dot{\epsilon}_r \quad (14)$$

$$\dot{\epsilon} = \dot{\epsilon}_r + \dot{\epsilon}_d \quad (15)$$

and

$$\ddot{\epsilon} = \ddot{\epsilon}_r + \ddot{\epsilon}_d \quad (16)$$

Substituting equations (13) (14) (15) (16) into (6), we get

$$M\ddot{q}_r + C_r\dot{q}_r + K_rq_r = D\delta + E\dot{\epsilon}_d + F\ddot{\epsilon}_d \quad (17)$$

where

$$q_r = \begin{pmatrix} y_r \\ \epsilon_r \\ \epsilon_f \end{pmatrix} \quad (18)$$

$$C_r = \frac{2}{\dot{x}} \begin{pmatrix} C_{\alpha f} + C_{\alpha r} + C_{\alpha t} & l_1 C_{\alpha f} - l_2 C_{\alpha r} - (l_3 + d_1) C_{\alpha t} - (m_1 + m_2) \dot{x}^2 & -l_3 C_{\alpha t} \\ l_1 C_{\alpha f} - l_2 C_{\alpha r} - (l_3 + d_1) C_{\alpha t} & l_1^2 C_{\alpha f} + l_2^2 C_{\alpha r} + (l_3 + d_1)^2 C_{\alpha t} + m_2 (d_1 + d_3) \dot{x}^2 & l_3 (l_3 + d_1) C_{\alpha t} + m_2 d_3 \dot{x}^2 \\ -l_3 C_{\alpha t} & l_3 (l_3 + d_1) C_{\alpha t} & l_3^2 C_{\alpha t} \end{pmatrix} \quad (19)$$

$$K_r = \begin{pmatrix} 0 & -2(C_{\alpha f} + C_{\alpha r} + C_{\alpha t}) & -2C_{\alpha t} \\ 0 & 2(-l_1 C_{\alpha f} + l_2 C_{\alpha r} + (l_3 + d_1) C_{\alpha t}) & 2(l_3 + d_1) C_{\alpha t} \\ 0 & 2l_3 C_{\alpha t} & 2l_3 C_{\alpha t} \end{pmatrix} \quad (20)$$

$$E = \frac{1}{\dot{x}} \begin{pmatrix} 2(-l_1 C_{\alpha f} + l_2 C_{\alpha r} + (l_3 + d_1) C_{\alpha t}) \\ -2(-l_1^2 C_{\alpha f} + l_2^2 C_{\alpha r} + (l_3 + d_1)^2 C_{\alpha t}) \\ m_2 d_3 \dot{x}^2 - 2l_3 (d_1 + l_3) C_{\alpha t} \end{pmatrix} \quad (21)$$

and

$$F = \begin{pmatrix} m_2 (d_1 + d_3) \\ -(I_{z1} + I_{z2} + m_2 (d_1^2 + d_3^2) + 2m_2 d_1 d_3) \\ -(I_{z2} + m_2 d_3^2 + m_2 d_1 d_3) \end{pmatrix} \quad (22)$$

We can further transform equation (17) into state space form. Defining $x_{6 \times 1} = (q^T, \dot{q}^T)^T$, then equation (17) can be written as

$$\begin{aligned} \frac{d}{dt} \begin{pmatrix} q \\ \dot{q} \end{pmatrix} &= \begin{pmatrix} 0 & I \\ -M^{-1}K_r & -M^{-1}C_r \end{pmatrix} \begin{pmatrix} q \\ \dot{q} \end{pmatrix} + M^{-1}D\delta + M^{-1}E\dot{\epsilon}_d + M^{-1}F\ddot{\epsilon}_d \\ &\equiv A x + B\delta + M^{-1}E\dot{\epsilon}_d + M^{-1}F\ddot{\epsilon}_d \end{aligned} \quad (23)$$

The state space form will be used in the design of linear controllers.

4.3 Open Loop Simulation

Figures 10, 11, 12 show the open loop responses of the linearized model (dotted line) and those of the complex nonlinear model (solid line). The longitudinal speed is fixed at 26.4 m/s (60 MPH) in these simulations, while the front wheel steering is a 3 degrees step input in figure 10, a 0.2 Hz sinusoidal input in figure 11, and a 0.3 Hz sinusoidal input in figure 12. In figure 10, the relative yaw angle between tractor and semitrailer achieves a steady state angle of 2 degrees when the steering is a step input. We also see from figure 11 and 12 that the vehicle performs a ‘‘lane change’’ when the sinusoidal steering input completes a cycle, which agrees with our driving experience.

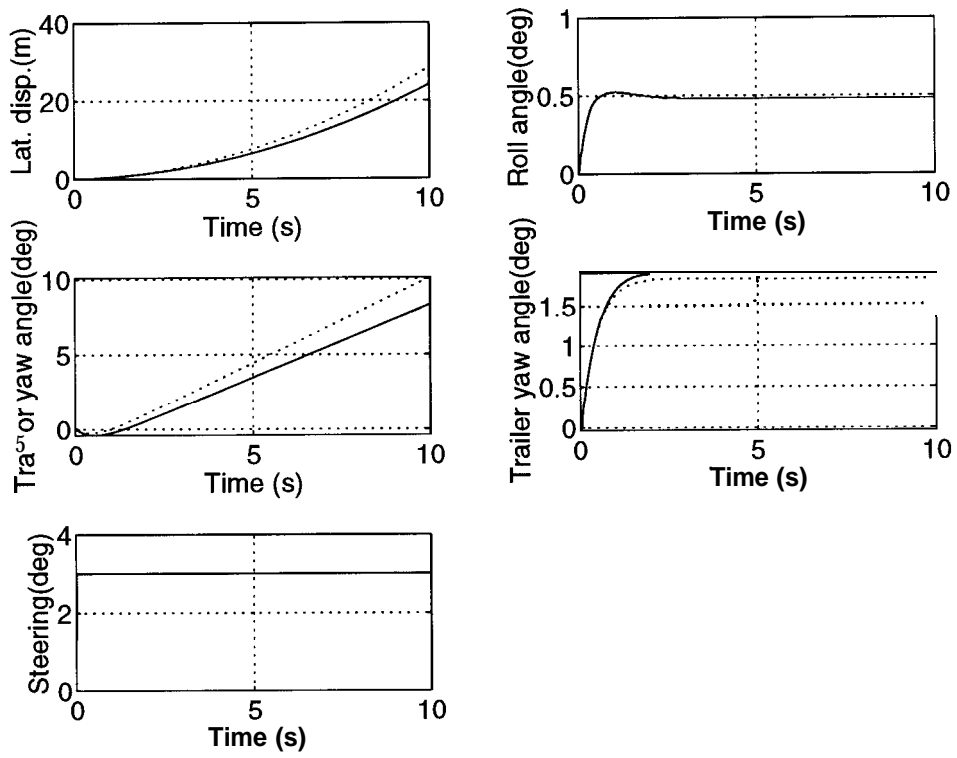


Figure 10: Step input response with the longitudinal vehicle speed 60 MPH

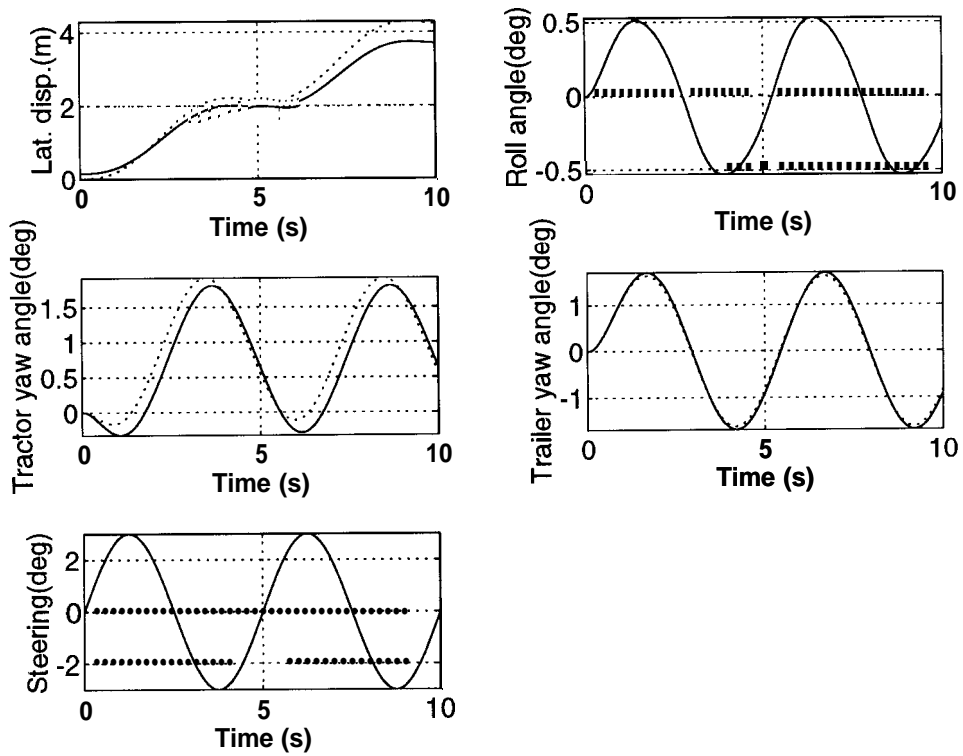


Figure 11: 0.2 Hz sinusoidal input response with the longitudinal vehicle speed 60 MPH

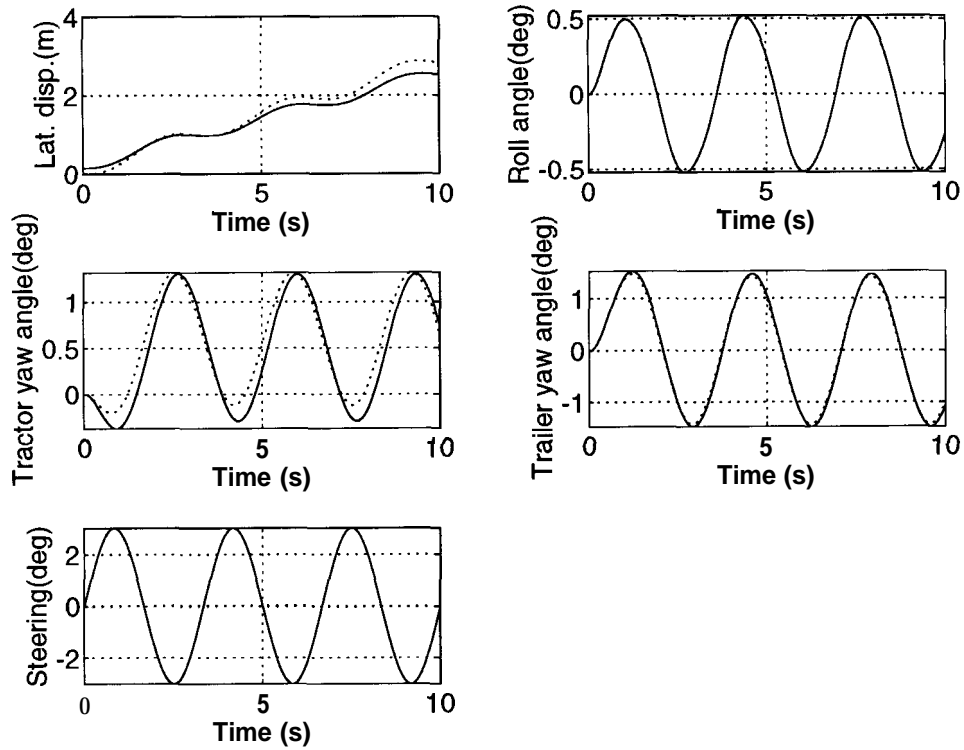


Figure 12: 0.3 Hz sinusoidal input response with the longitudinal vehicle speed 60 MPH

5 Concluding Remarks and Future Research

A nonlinear complex model for a tractor-semitrailer vehicle was formulated. This model was derived by applying Lagrangian mechanics and has an advantage over a Newtonian mechanics formulation in that our model eliminates the holonomic constraints at the fifth wheel by carefully choosing the generalized coordinates. Since there is no constraint involved in the equations of motion, it is easier to design control algorithms and to solve the differential equations numerically. Other configurations of articulated vehicles, for example tractor/three trailer combination, can also be modeled with the same approach. A linear control model was simplified from the complex nonlinear model. Linear quadratic optimal controller as well as nonlinear robust controllers will be designed based on this linear model in the near future.

6 Acknowledgment

This work is performed as part of Partners for Advanced Transit and Highways (PATH) program, prepared under the sponsorship of the State of California Business, Transportation, and Housing Agency, Department of Transportation.

Appendix 1

Nomenclature

δ : Tractor front wheel steering input.

\dot{x} : Longitudinal velocity of tractor unsprung mass coordinate relative to inertial reference coordinate.

\dot{y} : Lateral velocity of tractor unsprung mass coordinate relative to the inertial reference coordinate.

y_r, \dot{y}_r : Lateral displacement and lateral velocity of tractor unsprung coordinate relative to the road centerline coordinate.

z, \dot{z} : Vertical displacement and velocity of tractor unsprung mass relative to inertial reference coordinate.

$\phi, \dot{\phi}$: Roll angle and roll rate of tractor sprung mass coordinate relative to unsprung mass coordinate.

$\theta, \dot{\theta}$: Pitch angle and pitch rate of tractor sprung mass coordinate relative to unsprung mass coordinate.

$\dot{\epsilon}$: Yaw rate of tractor unsprung mass coordinate relative to the inertial reference coordinate.

$\dot{\epsilon}_d$: Desired yaw rate of the vehicle at curved section. If the radius of the curve is constant and equals to ρ , then $\dot{\epsilon}_d = \frac{\dot{x}}{\rho}$

$\epsilon_r, \dot{\epsilon}_r$: Yaw angle and yaw rate of the tractor relative to the road centerline coordinate, where $\dot{\epsilon}_r = \dot{\epsilon} - \dot{\epsilon}_d$.

$\theta_f, \dot{\theta}_f$: semitrailer pitch angle and pitch rate relative to tractor sprung mass coordinate.

$\epsilon_f, \dot{\epsilon}_f$: semitrailer yaw angle and yaw rate relative to tractor sprung mass coordinate.

α_i : Lateral slip angle at i -th wheel.

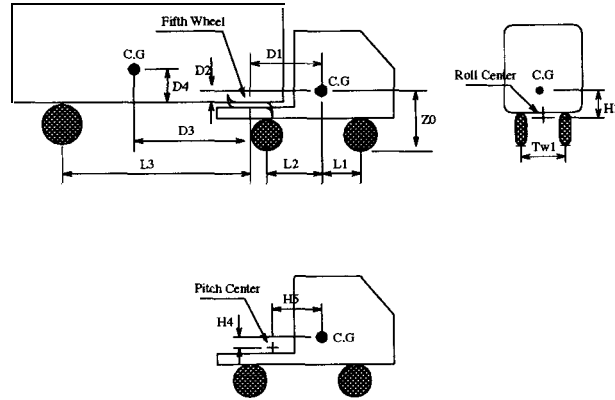


Figure 13: Vehicle Parameters

Vehicle parameters :

M_1 : tractor's mass.

I_{x1}, I_{y1}, I_{z1} : tractor mass of inertia.

M_2 : semitrailer's mass.

I_{x2}, I_{y2}, I_{z2} : semitrailer mass of inertia.

L_1 : distance from tractor C.G. to front wheel.

L_2 : distance from tractor C.G. to rear wheel.

L_3 : distance from fifth wheel to semitrailer wheel.

D_1, D_2 : relative position between tractor's C.G. to fifth wheel.

D_3, D_4 : relative position between semitrailer's C.G. to fifth wheel.

Tw_1 : tractor front axle track width.

Tw_2 : tractor rear axle track width.

Tw_3 : semitrailer rear axle track width.

Sw_1 : distance between the locations of tractor front axis suspension spring.

Sw_2 : distance between the locations of tractor rear axis suspension spring.

Sws : distance between the locations of semitrailer axis suspension spring.

H_2 : distance from tractor roll center to C.G.

H_4, H_5 : relative position between tractor pitch center and C.G.

Tire parameters :

$C_{\alpha f}$: cornering stiffness of tractor front wheel.

$C_{\alpha r}$: cornering stiffness of tractor rear wheel.

$C_{\alpha t}$: cornering stiffness of semitrailer rear wheel.

Sx_f : longitudinal stiffness of tractor front wheel.

Sx_r : longitudinal stiffness of tractor rear wheel.

Sx_t : longitudinal stiffness of semitrailer rear wheel.

Appendix 2

Transformation Matrices and Equations of Motion

$$R_u^s = \begin{pmatrix} 1 & 0 & -\theta \\ 0 & 1 & \phi \\ \theta & -\phi & 1 \end{pmatrix} \quad (24)$$

$$R_s^{pf} = \begin{pmatrix} 1 & 0 & -\theta_f \\ 0 & 1 & 0 \\ \theta_f & 0 & 1 \end{pmatrix} \quad (25)$$

$$R_{pf}^{yf} = \begin{pmatrix} \cos \epsilon_f & \sin \epsilon_f & 0 \\ -\sin \epsilon_f & \cos \epsilon_f & 0 \\ 0 & 0 & 1 \end{pmatrix} \quad (26)$$

$$\begin{aligned}
T_1 &= \frac{1}{2}m_1 \mathbf{X} (\dot{x} + h_4\dot{\theta} + h_2\dot{\phi}\dot{\epsilon})^2 \\
&+ \frac{1}{2}m_1 \mathbf{X} (\dot{y} + h_4\theta\dot{\epsilon} - h_2\dot{\phi})^2 \\
&+ \frac{1}{2}m_1 \mathbf{X} (\dot{z} - h_5\dot{\theta})^2 \\
&+ \frac{1}{2}I_{x1} \mathbf{X} (\dot{\phi} - \theta\dot{\epsilon})^2 \\
&+ \frac{1}{2}I_{y1} \mathbf{X} (\dot{\theta} + \phi\dot{\epsilon})^2 \\
&+ \frac{1}{2}I_{z1} \mathbf{X} (\dot{\epsilon})^2
\end{aligned} \tag{27}$$

$$V_1 = m_1g(z - h_5\theta) \tag{28}$$

$$\begin{aligned}
T_2 &= \frac{1}{2}m_2 \times \left(\begin{aligned} &(\dot{x} + h_6\dot{\theta} + h_3\phi\dot{\epsilon} - (\theta + \theta_f)\dot{z} - h_7(\theta + \theta_f)\dot{\theta} - \theta\theta_f\dot{x})\cos\epsilon_f \\ &+ (\dot{y} + h_6\theta\dot{\epsilon} - d_1\dot{\epsilon} - h_3\dot{\phi} + \phi\dot{z} + h_7\phi\dot{\theta})\sin\epsilon_f \\ &+ d_4(\dot{\theta} + \phi\dot{\epsilon} + \dot{\theta}_f)\cos\epsilon_f - d_4(\phi - \theta\dot{\epsilon} - \theta_f\dot{\epsilon})\sin\epsilon_f \end{aligned} \right)^2 \\
&+ \frac{1}{2}m_2 \times \left(\begin{aligned} &-(\dot{x} + h_6\dot{\theta} + h_3\phi\dot{\epsilon} - (\theta + \theta_f)\dot{z} - h_7(\theta + \theta_f)\dot{\theta} - \theta\theta_f\dot{x})\sin\epsilon_f \\ &+ (\dot{y} + h_6\theta\dot{\epsilon} - d_1\dot{\epsilon} - h_3\dot{\phi} + \phi\dot{z} + h_7\phi\dot{\theta})\cos\epsilon_f - d_3\theta_f\dot{\phi} - d_3(\dot{\epsilon} + \dot{\epsilon}_f) \\ &- d_4(\dot{\theta} + \phi\dot{\epsilon} + \dot{\theta}_f)\sin\epsilon_f - d_4(\phi - \theta\dot{\epsilon} - \theta_f\dot{\epsilon})\cos\epsilon_f \end{aligned} \right)^2 \\
&+ \frac{1}{2}m_2 \times \left(\begin{aligned} &\dot{z} + h_7\dot{\theta} - \phi\dot{y} + d_1\phi\dot{\epsilon} + h_3\phi\dot{\phi} + h_6(\theta + \theta_f)\dot{\theta} + (\theta + \theta_f)\dot{x} \\ &+ d_3(\dot{\theta} + \phi\dot{\epsilon} + \dot{\theta}_f)\cos\epsilon_f - d_3(\phi - \theta\dot{\epsilon} - \theta_f\dot{\epsilon})\sin\epsilon_f \end{aligned} \right)^2 \\
&+ \frac{1}{2}I_{x2}((\dot{\phi} - (\theta + \theta_f)\dot{\epsilon})\cos\epsilon_f + (\phi\dot{\epsilon} + \dot{\theta} + \dot{\theta}_f)\sin\epsilon_f)^2 \\
&+ \frac{1}{2}I_{y2}(-(\dot{\phi} - (\theta + \theta_f)\dot{\epsilon})\sin\epsilon_f + (\phi\dot{\epsilon} + \dot{\theta} + \dot{\theta}_f)\cos\epsilon_f)^2 \\
&+ \frac{1}{2}I_{z2}(\theta_f\dot{\phi} + \dot{\epsilon} + \dot{\epsilon}_f)^2
\end{aligned} \tag{29}$$

$$V_2 = m_2g(z + h_7\theta + d_3(\theta + \theta_f)\cos\epsilon_f - d_3\phi\sin\epsilon_f) \tag{30}$$

$$L = T - V \tag{31}$$

From Lagrange's equation, we get:

$$\frac{d}{dt} \frac{\partial L}{\partial \dot{x}_1} - \frac{\partial L}{\partial x_1} = F_x \tag{32}$$

$$\frac{d}{dt} \frac{\partial L}{\partial \dot{y}_1} - \frac{\partial L}{\partial y_1} = F_y \tag{33}$$

$$\frac{d}{dt} \frac{\partial L}{\partial \dot{z}_1} - \frac{\partial L}{\partial z_1} = F_z \tag{34}$$

$$\frac{d}{dt} \frac{\partial L}{\partial \dot{\phi}_1} - \frac{\partial L}{\partial \phi_1} = M_\phi \tag{35}$$

$$\frac{d}{dt} \frac{\partial L}{\partial \dot{\theta}_1} - \frac{\partial L}{\partial \theta_1} = M_\theta \tag{36}$$

$$\frac{d}{dt} \frac{\partial L}{\partial \dot{\epsilon}_1} - \frac{\partial L}{\partial \epsilon_1} = M_\epsilon \tag{37}$$

$$\frac{d}{dt} \frac{\partial L}{\partial \dot{\theta}_f} - \frac{\partial L}{\partial \theta_f} = M_{\theta_f} \quad (38)$$

$$\frac{d}{dt} \frac{\partial L}{\partial \dot{\epsilon}_f} - \frac{\partial L}{\partial \epsilon_f} = M_{\epsilon_f} \quad (39)$$

Appendix 3

Generalized Forces for the Equations of Motion

$$F_x = F_{A1} + F_{A2} + F_{A3} + F_{A4} + F_{A5} + F_{A6} \quad (40)$$

$$F_y = F_{B1} + F_{B2} + F_{B3} + F_{B4} + F_{B5} + F_{B6} \quad (41)$$

$$F_z = F_{P1} + F_{P2} + F_{P3} + F_{P4} + F_{P5} + F_{P6} \quad (42)$$

$$M_\phi = (\sum_{i=1}^6 F_{Bi})(z_0 - h_2) + (F_{P1} - F_{P2})\frac{Sw1}{2} + (F_{P3} - F_{P4})\frac{Sw2}{2} + F_{P5}(\frac{Sw3}{2}\cos\epsilon_f - l_3\sin\epsilon_f) + F_{P6}(-\frac{Sw3}{2}\cos\epsilon_f - l_3\sin\epsilon_f) \quad (43)$$

$$M_\theta = -(\sum_{i=1}^6 F_{Ai})(z_0 - h_4) - (F_{P1} + F_{P2})(l_1 + h_5) + (F_{P3} + F_{P4})(l_2 - h_5) + F_{P5}(l_3\cos\epsilon_f + \frac{Sw3}{2}\sin\epsilon_f + h_7) + F_{P6}(l_3\cos\epsilon_f - \frac{Sw3}{2}\sin\epsilon_f + h_7) \quad (44)$$

$$M_\epsilon = (F_{A2} - F_{A1})\frac{Sw1}{2} + (F_{A4} - F_{A3})\frac{Sw2}{2} + F_{A5}(-\frac{Sw3}{2}\cos\epsilon_f + l_3\sin\epsilon_f) + F_{A6}(\frac{Sw3}{2}\cos\epsilon_f + l_3\sin\epsilon_f) + (F_{B1} + F_{B2})l_1 - (F_{B3} + F_{B4})l_2 + F_{B5}(-\frac{Sw3}{2}\sin\epsilon_f - l_3\cos\epsilon_f - d_1) + F_{B6}(\frac{Sw3}{2}\sin\epsilon_f - l_3\cos\epsilon_f - d_1) \quad (45)$$

$$m_{e_r} = -(F_{A5} + F_{A6})(z_0 - d_2) + F_{P5}(l_3\cos\epsilon_f + \frac{Sw3}{2}\sin\epsilon_f) + F_{P6}(l_3\cos\epsilon_f - \frac{Sw3}{2}\sin\epsilon_f) \quad (46)$$

$$M_{\epsilon_f} = F_{A5}(l_3\sin\epsilon_f - \frac{Sw3}{2}\cos\epsilon_f) + F_{A6}(l_3\sin\epsilon_f + \frac{Sw3}{2}\cos\epsilon_f) + F_{B5}(-l_3\cos\epsilon_f - \frac{Sw3}{2}\sin\epsilon_f) + F_{B6}(-l_3\cos\epsilon_f + \frac{Sw3}{2}\sin\epsilon_f) \quad (47)$$

Appendix 4

Tire Longitudinal Slip Ratios and Lateral Slip Angles for (i-wheel tractor-semitrailer vehicle

The longitudinal slip ratio, λ_i , is equal to

$$\lambda_i = \frac{V_i - \omega_i r_i}{V_i} \text{ for braking}$$

and

$$\lambda_i = \frac{\omega_i r_i - V_i}{\omega_i r_i} \text{ for traction}$$

where V_i is the forward velocity, ω_i is the angular velocity and r_i is the radius of the i -th wheel.

The lateral slip angle, α_i , is equal to

$$\alpha_1 = \delta - \tan^{-1} \left(\frac{\dot{y} + l_1 \dot{\epsilon}}{\dot{x} - \frac{Tw1}{2} \dot{\epsilon}} \right), \quad (48)$$

$$\alpha_2 = \delta - \tan^{-1} \left(\frac{\dot{y} + l_1 \dot{\epsilon}}{\dot{x} + \frac{T_w1}{2} \dot{\epsilon}} \right), \quad (49)$$

$$\alpha_3 = -\tan^{-1} \left(\frac{\dot{y} - l_2 \dot{\epsilon}}{\dot{x} - \frac{T_w2}{2} \dot{\epsilon}} \right), \quad (50)$$

$$\alpha_4 = -\tan^{-1} \left(\frac{\dot{y} - l_2 \dot{\epsilon}}{\dot{x} + \frac{T_w2}{2} \dot{\epsilon}} \right), \quad (51)$$

$$\alpha_5 = -\tan^{-1} \left(\frac{-\dot{x} \sin \epsilon_f + (\dot{y} - d_1 \dot{\epsilon}) \cos \epsilon - l_3 (\dot{\epsilon} + \dot{\epsilon}_f)}{\dot{x} \cos \epsilon_f + (\dot{y} - d_1 \dot{\epsilon}) \sin \epsilon_f - \frac{T_w3}{2} (\dot{\epsilon} + \dot{\epsilon}_f)} \right) \quad (52)$$

and

$$\alpha_6 = -\tan^{-1} \left(\frac{-\dot{x} \sin \epsilon_f + (\dot{y} - d_1 \dot{\epsilon}) \cos \epsilon - l_3 (\dot{\epsilon} + \dot{\epsilon}_f)}{\dot{x} \cos \epsilon_f + (\dot{y} - d_1 \dot{\epsilon}) \sin \epsilon_f + \frac{T_w3}{2} (\dot{\epsilon} + \dot{\epsilon}_f)} \right) \quad (53)$$

Appendix 5 Suspension Deflections

$$e_1 = l_1 \theta - \frac{Sw1}{2} \phi + z \quad (54)$$

$$e_2 = l_1 \theta + \frac{Sw1}{2} \phi + z \quad (55)$$

$$e_3 = -l_2 \theta - \frac{Sw2}{2} \phi + z \quad (56)$$

$$e_4 = -l_2 \theta + \frac{Sw1}{2} \phi + z \quad (57)$$

$$e_5 = -(l_3 (\theta + \theta_f) + \frac{Sw3}{2} \phi) \cos \epsilon_f - \left(\frac{Sw3}{2} \theta - l_3 \phi + \frac{Sw3}{2} \theta_f \right) \sin \epsilon_f - h_7 \theta - z \quad (58)$$

$$e_6 = -(l_3 (\theta + \theta_f) - \frac{Sw3}{2} \phi) \cos \epsilon_f + \left(\frac{Sw3}{2} \theta + l_3 \phi + \frac{Sw3}{2} \theta_f \right) \sin \epsilon_f - h_7 \theta + z \quad (59)$$

References

- Baraket, Z., and P. Fancher. 1989. "Representation of Truck Tire Properties in Braking and Handling Studies: The Influence of Pavement and Tire Conditions on Frictional Characteristics.", Technical Report, University of Michigan, Ann Arbor, UMTRI-89-33.
- Bundorf, R.T. 1967. "Directional Control Dynamics of Automobile-Travel Trailer Combinations", **SAE Transactions**, Vol. 76, SAE paper No. 670099.
- Chee, W., and M. Tomizuka. 1994. "Lane Change Maneuvers", *Proceedings of American Control Conference*, Baltimore.
- Dugoff, H., and R.W.Murphy. 1971. "The Dynamic Performance of Articulated Highway Vehicles - A review of the State-of-the-Art", **SAE Transactions**, SAE paper no. 710223.
- Ellis J.R. 1989. **Road Vehicle Dynamics**, 2nd impression.
- Hessburg, T., and M.Tomizuka. 1993. "Fuzzy Logic Controller for Lateral Vehicle Guidance", **IEEE Conference on Control Applications**, Vancouver, Canada.
- Huang, F. et al. 1993. "The Use of Random Steer Test Data for Vehicle Parameter Estimation", Presented in 1993 SAE Congress and Exposition, Detroit, MI, SAE paper no. 930830.
- Motor Vehicle Manufactureers Association of The United States (MVMA). 1987. *Motor Vehicle Facts and Figures*.
- Motor Vehicle Manufactureers Association of The United States (MVMA). 1992. **World Motor Vehicle Data**.
- Peng, H., Tomizuka, M. 1991. "Preview Control for Vehicle Lateral Guidance in Highway Automation", **Proceedings of American Control Conference**, Boston.
- Peng, H. et al. 1992. "A Theoretical and Experimental Study on Vehicle Lateral Control", **Proceedings of American Control Conference**, Chicago.
- SAE Spring Committee (SAE). 1982. "Manual on Design and Application of Leaf Springs- SAE J788a." **SAE Information Report**, 4th Edition.
- Vlk, F. 1982. "Lateral Dynamics of Commercial Vehicle Combinations - A Literature Survey", **Vehicle System Dynamics**, Vol. 11, pp.305-324.
- Vlk, F. 1985. "Handling Performance of Truck-Trailer Vehicles: A State-of-the-art Survey", **International Journal of Vehicle Design**, Vol.1.6, No.3, pp322-361.
- Zhang,W. et al. 1990. "An Intelligent Roadway Reference System for Vehicle Lateral Guidance/Control", **Proceedings of American Control Conference**, San Diego.